EPJ Web of Conferences **6**, 04004 (2010)
DOI:10.1051/epjconf/20100604004

Friction measurements on carbon fibre tows

B. Cornelissen[a], L. Warnet, and R. Akkerman

University of Twente, Department of Mechanical Engineering, Chair of Production Technology, P.O. box 217, 7500 AE Enschede, the Netherlands

Abstract. Friction plays an important role in the production of fibre reinforced composite products. The fibrous tows deform during the forming phase. Friction is regarded as a dominant phenomenon in tow deformation mechanisms. The coefficient of friction is a material-interface characteristic which gives a relation between applied deformation loads and frictional forces. A capstan experiment has been performed with carbon fibre tows on a steel cylinder. This work aims to clarify friction related mechanisms and identify dominant parameters. The applicability of the capstan experiment is investigated with respect to the frictional behaviour of fibrous tows.

1 Introduction

The mechanical properties of continuous fibre reinforced polymers or composite parts are determined to a large extent during the forming phase. Such composite products consist of a thermosetting or thermoplastic matrix, which is reinforced with continuous fibrous tows (a tow consists of several thousands of filaments). The continuous fibrous tows deform during the forming phase of any arbitrary production technique involving fibrous material. The tows conform to the local shape of the tool surface. Local cross-sectional changes in the tow occur due to the induced loads. Fibre orientation and redistribution determine to a large extent the properties of a composite product. Knowledge of the tow orientation and tow deformation behaviour is therefore essential to control the desired product quality in terms of e.g. mechanical performance and shape preservation. Composite products can be

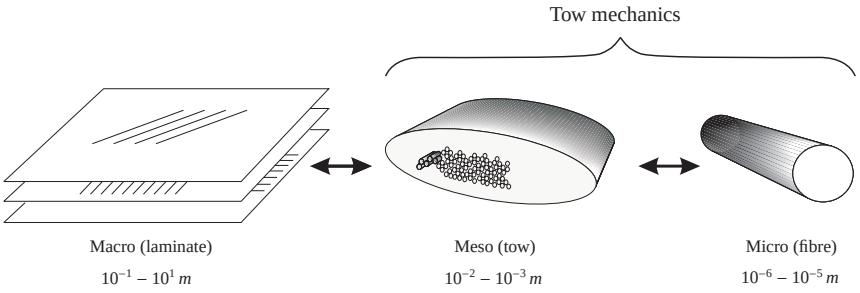

Fig. 1. Macro-meso-micro hierarchical structure of composite materials (with characteristic length scales).

represented in a hierarchical structure. A classification is made in three scales, as illustrated in figure 1: macro, meso, and micro to represent the product, tow, and filament scale, respectively. The frictional properties of fibrous tows are examined on the combined meso-micro scale. The frictional behaviour of individual carbon filaments (on the micro scale) was investigated in earlier research [1,2]. The

[a] e-mail: b.cornelissen@utwente.nl

hierarchical approach does not imply that deformation mechanisms are isolated on a single scale level. For example, fibres moving relatively to each other within a tow on the micro level will result in a change in cross-sectional properties of the tow on the meso level. Meso and macro scale effects are interrelated as well. An example is the formation of wrinkles in a doubly curved rubber pressed composite product due to tow orientation dependent inter-ply friction and shear [3].
Previous modelling efforts of forming processes, in which macro and meso effects are related to each other, show that friction mechanisms are an important factor in the deformation behaviour of tows and plies [3–5]. One can for instance account for friction on the macro level by assuming a lubricated contact with mesoscopic information [6]. Knowledge of the meso-micro scale interactions is needed, to incorporate friction mechanisms on the meso scale. A physically sound model based on elementary deformation mechanisms is expected to provide the required information.
The deformations that occur in the forming phase of composite products induce loads on the tows and fibres. This results in frictional forces at different interfaces. The determination of the involved friction mechanisms of the tows and fibres with respect to each other and mould materials such as tooling steel is necessary to accurately predict the tow deformation in the dry and impregnated fabric, individual tow, and tape material. We define this area as 'tow mechanics', aiming to develop a theoretical approach which covers the wide range of loading conditions encountered during composite processing. Experimental work is necessary to obtain the physical basis for this theoretical approach.

2 Tow Mechanics

The study of meso-micro interactions is based on a break-down of an arbitrary process-induced load into more specific simple loading mechanisms. A characterisation of tow deformation behaviour by means of distinct load mechanisms is proposed. This results in a set of five individual load mechanisms which cover the tow deformation behaviour during forming processes on the meso and micro scale, thereby affecting related mechanisms on the macro scale as well:

1. **Tension:** A load is applied in axial direction with respect to the local tow or fibre axes.
2. **Compaction:** A load is applied perpendicular to the longitudinal axes of the tows or fibres.
3. **Bending:** A moment is induced in a tow or fibre section (the case of tow bending behaviour is described in previous work [7]).
4. **Twist:** Torsion due to a relative rotation between two locations is applied along the longitudinal axis on the tows or fibres. Sliding between the fibres or tows is expected to occur either in or transverse to the fibre direction.
5. **Shear:** A load is induced by a relative displacement of two parallel planes, which remain parallel during and after the displacement. The shear mechanism can be decomposed into a longitudinal and transverse component with respect to the fibre axis.

Of these five mechanisms, only tension has no straightforward relation with friction. The four remaining mechanisms are expected to be related to friction, depending on load type, tow or fibre orientation and interface type. Friction can therefore be considered a dominant factor in characterising the forming phase of composite materials. Here, we investigate the friction properties of fibrous tows before addressing the proposed mechanisms individually.

3 Dry friction

The most simple form of friction is dry friction, where two material interfaces are directly in contact with each other. The term *dry* in this context refers to the absence of a lubricating film between the two interacting materials. Many friction characterisation studies were performed in the twentieth century, a large number originates from processes in the textile industry. An overview was produced recently by Yuksekkaya in [8]. Different measurement methods were proposed of which the capstan method is one of the most straightforward and versatile methods. Previous efforts to characterise friction behaviour of carbon fibre material by means of the capstan relation focused on single fibres [2, 9]. This research

focuses on applying the capstan approach to dry tow material, which consists of several thousands of filaments. In this case, the dominant tow deformation mechanisms are tension and bending. The other three mechanisms outlined in section 2 are expected to have a minor contribution in this experiment.
Amontons analysed friction by means of the simple capstan experiment, as illustrated by figure 2, in the seventeenth century. The capstan equation proposed by Amontons (Eq. 1) relates tensional forces T_1 and T_2 in the ends of a tow to the friction coefficient μ and the angle of contact θ of the tow with a cylindrical surface:

$$\mu = ln\left(\frac{T_2}{T_1}\right)\frac{1}{\theta} \tag{1}$$

Several assumptions are made in this relation. The friction coefficient μ is assumed to remain constant, so load and contact area dependence are neglected. The use of this simplified relation is attractive due to the absence of fitting parameters and the possibility to compare results under varying conditions. This paper treats preliminary friction measurements on dry carbon fibre tows on a steel surface to establish relevant parameters for the description of tow deformation behaviour.

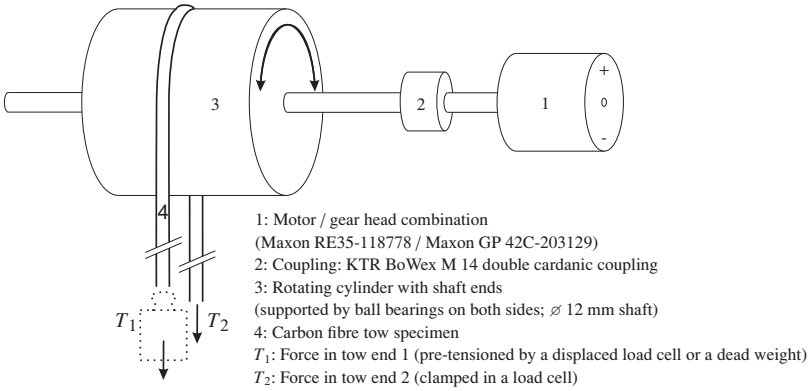

Fig. 2. Schematic description of the capstan experiment for carbon fibre tows.

4 Experimental work

4.1 Set-up description

A capstan type measurement set-up was designed (figure 2), based on the ASTM D3108-07 [10] and ASTM D3412-07 [11] standard test methods. A tow specimen is draped with an angle of π radians across a metal cylinder. The cylinder and shaft are machined from one single part and the shaft ends are fitted with ball bearings, which are supported by mounts on a single aluminium base plate. One end of the cylinder shaft is connected to a motor / gear head combination with a cardanic coupling in between to compensate possible radial and angular alignment errors between motor and cylinder as much as possible. The motor support is mounted on the same base plate as the bearing supports. This part of the set-up is mounted approximately 40 cm above an aluminium slab on which two load cells [1] equipped with clamps are mounted. One of the load cells is mounted in a vertically movable structure (micrometer controlled, range 50, 0 mm) to enable pre-tensioning of the tow specimen.

[1] HBM SP4C3-MR single point load cells (range: 0 – 30 N)

Table 1. Experimental parameters

Parameter	Type	Value	Unit
Tow material	T300J B carbon	198 (3 k, 7 μm $fibres$)	tex
	T800H B carbon	445 (12 k, 5 μm fibres)	tex
Counter face cylinder material	Steel	30CrNiMo8	-
Counter face cylinder diameter		50	mm
Counter face cylinder roughness	Ra	0.01	μm
Tow draping angle on cylinder		π	$radians$
Rotational frequency		0.11 ± 0.1	Hz
		0.21 ± 0.1	Hz
Corresponding sliding velocity		17.3	$mm \cdot s^{-1}$
		33.0	$mm \cdot s^{-1}$
Dead weight	At one tow end	319.9 ± 0.1	$gram$
		500.0 ± 0.1	$gram$

4.2 Friction coefficient

The friction coefficient μ is calculated from the logged tensional forces T_1 and T_2 at the tow ends with equation 1. The fibrous tow material used in the experimental part of this research is not impregnated, but might contain small amounts of sizing due to incomplete cleaning. The fibrous tow material went through a thermal cleaning process, in which the sizing was burned off almost completely. The remaining amount of sizing is very small, a maximum amount of 0.01 % mass, instead of the initial 1 % mass is present. Therefore, the friction is considered dry. Any sizing remains are expected to wear off in the first part of the performed measurement sessions.

4.3 Measurement procedure

The experimental parameters are presented in table 1. The ambient temperature and humidity were logged during the measurements. The temperatures during the experiments ranged from 20.5 °C to 22.4 °C (±0.1 °C), and humidities between 15.6% RH and 37.1 % RH (± 0.1 % RH) were measured.
Every measurement session was performed in two runs with one specimen. Two methods were used to apply the load on the fibrous tow specimen:

1. using a dead weight on one of the ends, free to rotate and move laterally
2. using the fixed clamp to exert tension by means of a fixed downward displacement of the pre-tensioning device

The cylinder was cleaned before each measurement session with an acetone impregnated paper cloth and a 3 k or 12 k tow specimen was draped over the cylinder. The tow specimen remained clamped between the first and second measurement run, yet it was lifted from the cylinder and put back again. In the first load case this meant that the weight was lifted to enable the tow specimen to be removed from the cylinder. In the second case, the movable load cell holder was displaced upward to remove the pre-tension. The load cell carrier could be displaced further upward to give the tow specimen enough room to be removed from the cylinder surface. The effect of this procedure was that the tow specimen was ‘relieved’ and a new static friction situation could be established for the second measurement run. The preliminary character of this research implies that no effort is made to obtain statistically relevant results. Many parameters were varied, sometimes more than one at the same time. The amount of measurements could hereby be kept to a minimum. The metal cylinder, whose properties are stated in table 1, is used for all described measurements.

5 Results and discussion

The graphs presented in figure 3 form an illustration of the obtained preliminary experimental results. The following subsections discuss observed trends and form a starting point for further experimental work.

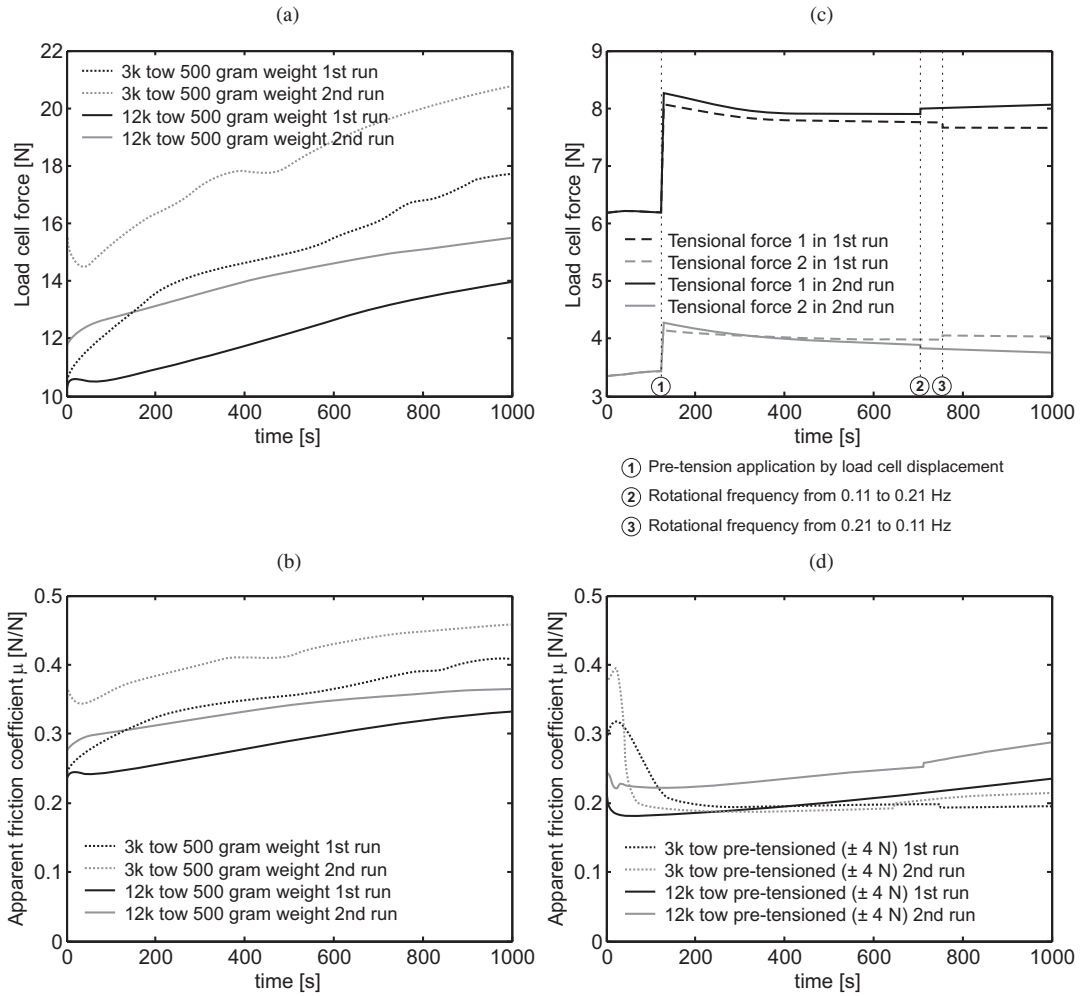

Fig. 3. Time-dependence of the apparent friction coefficients for the dead weight loading case and the pre-tensioned case. In (a) the Force-time relation of the measured load is plotted for the 500 gram dead weight. Graph (b) shows the friction coefficient with time for the 500 gram dead weight. Graph (c) shows a typical force-time relation for the pre-tensioned specimen. Both tow ends are connected to load cells. The ratio between tensional force 1 and 2 determines the apparent friction coefficient. The non-zero forces between 0 s and approximately 120 s in graph (c) represent the weight load of the movable load cell carrier. Graph (d) shows the apparent friction coefficient as a function of time for four measurements in the pre-tensioned loading case. The cylinder rotation started at approximately 0 s for all measurements.

5.1 Time dependence

All measurements showed that the forces in the tow end(s) were varying with time, regardless of the loading case. Figure 3 shows typical measurement results in terms of forces and calculated apparent friction coefficients. The change in frictional forces with time is clearly visible, yet the scale on which changes occur is larger than the present 1000 s time frame. This scale is large enough to show that the friction coefficient μ (calculated with eq. 1) is not constant with time. Several longer measurements have been performed, but a constant μ has not been observed, even after 8 hours. The authors expect wear of the specimen to play a significant role in the change of the friction coefficient on the long term (in one case a peak of μ was observed after $\pm$ 6200 s, followed by a gradual decrease) . Therefore, a constant μ will probably never be observed. The time scale on which tow specimens are deformed during an actual forming process is much smaller than 1000 s, which puts the time scale discussion into a rather academic perspective.
Possible causes for the increase in measured forces, and consequently an increase in the apparent friction coefficient with time, are described in the following subsections.

5.2 Dead weight load versus pre-tensioned load

The apparent friction coefficients for the pre-tension loading case are significantly lower than for the 500 gram dead weight loading case, as illustrated by figures 3(b) and 3(d). The applied pre-tensional force is lower than the tensional force from the dead weight, but other measurements with a 320 gram dead load weight showed friction coefficients in the same range as the 500 gram dead load measurements. The difference in absolute forces is therefore not expected to cause the observed discrepancy.
There is, however, a difference between the two types of loading cases in allowed degrees of freedom of the tow ends. The tow end carrying the dead weight has the freedom to shift sidewards (in the direction of the cylinder axis) and the free part of the tow end between the cylinder surface and the weight can rotate freely. Shifting of the specimen is possible in the pre-tension loading case as well, but to a lesser extent. Shifting causes an increase in tensional force, which is not the case for the dead weight load. The freedom of rotation of the pre-tensioned specimen is inhibited by the two clamps in contrast to the dead weight loading case where only one clamp is used.
The tow specimens flattened in both cases on the cylinder contact surface due to normal load. The combination of the frictional forces at the cylinder-specimen interface and the normal loads due to the tensional forces in the tow ends most likely caused the fibres to displace with respect to each other. The observed presence of (unintended) twist in the specimens is another factor affecting the rearrangement of fibres. The visible part of the bottom side of the tow specimen that was in contact with the cylinder showed that fibres were displaced in a rather chaotic manner, with small bundles of fibres running diagonally across each other in the width direction of the tow. The orientation of the visible fibres on the top side of the specimen, which was not in contact with the cylinder surface, looked more like the initial specimen state before the measurement was conducted. Here, the fibres had a more parallel orientation and appeared less disturbed. The dead weight showed small rotational movement during the measurements, this might indicate another fibre reorientation system than for the pre-tensioned loading case.
The capstan equation (eq. 1) does not account for the different loading cases, there is no matter of a wrong or right type of load application. The load mechanisms involved in the capstan experiment are the same for both loading case types: the specimen is bent along the curved cylinder surface, compaction occurs at the contact region due to the normal load, induced by the tensional forces in the tow ends, fibres are loaded in shear when displacing relatively to each other, and twist in the tow is a factor that affects the rearrangement of fibres. Isolation of individual loading mechanisms might offer an explanation for the observed load case dependent behaviour. Additional experiments have to be performed to gather information for the isolated mechanisms.

5.3 First versus second measurement run

The apparent friction coefficient was higher for the second run than for the first in almost every measurement, regardless of the loading case or tow specimen type (see figure 3(a)-3(c)). The difference can possibly be caused by the small amount of remaining sizing on the specimens, as mentioned before in section 4. The sizing might have formed a film between the tow specimen and the cylinder surface, although the amount of present sizing was minimal. The cylinder was not cleaned between two runs, which means that any deposit on the cylinder was not removed by a wiping action. Further measurements with more than two runs per specimen will be performed to gain insight in this phenomenon.

5.4 Tow type

Two different tow types were used in this experiment (specifications in table 1). The amount of fibres in the tows was different as well as the fibre diameter and material type (the reported tensile strengths are 4210 MPa and 5490 MPa; tensile moduli of 230 GPa and 294 GPa for the T300J and T800H tows respectively). Therefore, it is difficult to draw conclusions related to the contact area of the specimens on the cylinder surface. Differences in apparent friction coefficient between 3 k and 12 k tows can possibly be related to other properties than the number of fibres in the tow. There is, however, a large difference in measured apparent friction coefficients between the two different tow types used in this experiment. This difference is more apparent in the dead weight than in the pre-tension loading case. The fact that in the dead weight loading case the 3 k tows show a higher apparent friction coefficient than the 12 k tows and vice versa in the pre-tension loaded case is remarkable as well. More experiments have to be performed to gain insight in this behaviour. Experiments with tow specimens of the same type but different yield and several pre-tension values can give an insight in the relation between the apparent friction coefficient and the normal pressure on the tow specimen. Results can be analysed with an adhesion/ploughing model, e.g. the one proposed by Roselman and Tabor in [1].

5.5 Rotational velocity

The effect of rotational velocity on the apparent friction coefficient was not studied in detail. Two different rotational velocities, stated in table 1, were applied in the pre-tension loading case measurements. The effect of velocity on the apparent friction coefficient is rather limited for the values used in this experiment, this is illustrated by the circled numbers 2 and 3 by graphs (c) and (d) in figure 3. The apparent friction coefficient increased with a rise and vice versa for a drop in rotational velocity. The velocities have to be varied in a range of several decades to obtain a more complete relation between the rotational velocity and friction behaviour.

5.6 Environmental factors

The measurements were performed in a lab where the environmental conditions were monitored. The room temperature was controlled between 20.5 °C and 22.4 °C (±0.1 °C), the ambient conditions determined the relative humidity during the measurements. Carbon fibre material is known to be sensitive to environmental humidity and it is therefore advisable to perform experiments in which the relative humidity and moisture uptake of the specimens are varied intentionally to establish a relation between environmental conditions and frictional behaviour of the tow specimens.

5.7 Cylinder material

A steel cylinder with a single roughness was used during the experiment. The frictional behaviour of fibrous tows is expected to vary with the roughness of the counter-face material. The

adhesion/ploughing relation mentioned in subsection 5.4 takes varying roughness values into account. Other counter-face materials such as fibrous tows will be tested as well, since tow-tow interactions are always present in the processing of composites.

6 Conclusion

The measurement of friction between fibrous tows and a steel counter-face is possible with the capstan method, but the simple relation between loads in the tow ends and the friction coefficient proposed by Amontons is not valid in case of carbon fibre tow material in contact with typical forming tool steel. The performed experiments did not yield unique friction coefficients for every described material-counter-surface combination. Calculated apparent friction coefficients showed a dependence on time, tow material, environmental conditions and type of load application. The capstan method is nevertheless a practical experiment, which gives the possibility to establish relevant parameters related the frictional behaviour of dry carbon fibre tows on steel. Further research has to be performed to explain the measured force fluctuations. This can be achieved by conducting experiments in which the discussed parameters are isolated and brought into relation with the distinct loading mechanisms described in this paper.

References

1. I.C. Roselman, D. Tabor, J. of Phys. D: Appl. Phys. **9**, (1976) 2517–2532
2. I.C. Roselman, D. Tabor, J. of Phys. D: Appl. Phys. **10**, (1977) 1181–1194
3. R. ten Thije, *Finite element simulations of laminated composite forming processes*, (University of Twente, Enschede, 2007) 67–84
4. P. Boisse, B. Zouari, A. Gasser, Compos. Sci. Technol. **65**, (2005) 429–436
5. S.V. Lomov, I. Verpoest, Compos. Sci. Technol. **66**, (2006) 919–933
6. R. ten Thije, R. Akkerman, L. van der Meer, M. Ubbink, Int. J. Mater. Form. **1**, (2008) 953–956
7. B. Cornelissen, R. Akkerman, *Proc. 17th Int. Conf. on Composite Materials (ICCM 17)*, Edinburgh, Scotland, 2009
8. M.E. Yuksekkaya, Text. Prog., **41**, (2009) 141–193
9. M.M. Robins, R.W. Rennell, R.D. Arnell, J. of Phys. D: Appl. Phys. **17**, (1984) 1349–1360
10. ASTM D3108-07: Standard test method for coefficient of friction - yarn to solid material (2007)
11. ASTM D3412-07: Standard test method for coefficient of friction - yarn to yarn (2007)